Slingshot disconnection! Understanding the effect of disconnecting an un-stabilized ungrounded source

Sebastien Billaut PE[1]
James Steele EIT [2]
Joseph Johnson PE[2]
System Protection and Analysis
Commonwealth Associates, Inc.
[1] Lake Mary, Florida, USA
[2] Jackson, Michigan, USA

Stephen Miller, PE
Energy Emissions Intelligence
Ann Arbor, Michigan, USA

Koustubh Banerjee, PE
Transmission System Planning
Eversource Energy, Inc.
Westwood, Massachusetts, USA

***Abstract*— The IEEE C37.234 [1] guide is important for protection and control engineers looking to implement bus protection. Within this framework, Section 8.3 addresses bus protection and details using a broken delta-configured PT and stabilizing resistors to mitigate large overvoltage on ungrounded systems and to assist in detecting ground faults. This paper investigated the sizing and impact of these elements on ungrounded systems using an Electro-Magnetic Transient (EMT) program. This paper also explored the phenomenon we call the "voltage slingshot" effect.**

Unbalanced capacitance within a power system can lead to asymmetric voltage distribution and transient instability. The incorporation of stabilizing resistors can be used to mitigate these issues. Section 8.3 of IEEE C37.234 [1] describes the impact of broken delta-configured PTs connected to a stabilizing resistor and the existing industry practice for sizing them. We investigated the efficacy of this setup using EMT software with different magnitudes of capacitance imbalance on a system. We concluded those situations that warranted or precluded a broken delta/stabilizing resistor as an effective solution to system imbalance. We created an equation describing the relationship between capacitance imbalance and zero sequence voltage/stabilizing resistor current flow.

Furthermore, this paper explored the voltage slingshot effect, which arises during rapid breaker reclosing onto a capacitive system. Such actions can cause voltage levels to surge well beyond 5 per unit, potentially compromising the insulation and protective devices. Understanding the mechanisms behind this effect is paramount to ensuring the reliable operation of power systems.

In conclusion, this paper highlights the significance of Section 8.3 in IEEE C37.234 [1], emphasizing the need to address the impacts of broken delta and stabilizing resistors on systems with imbalanced capacitance. It underscores the importance of safeguarding against the voltage slingshot effect to maintain system stability and reliability in the face of electric transient disturbances.

***Index Terms*—Bus protection, Broken-delta, Overvoltage, Ungrounded.**

I. INTRODUCTION

Ungrounded sources, by design or by unexpected circumstances, had puzzled system operators until analysis and testing were performed between 1931 and the 1950s [2] [3] [4]. Most of this research studied the effect of the ferro-resonance caused when the ratio of impedance presented by the bus shunt capacitance to the primary phase to ground PT's magnetic impedance (Xco/Xm) becomes large which in turn creates instability regions. To prevent this, a load resistor on the secondary of a broken delta connected PT must be sized to keep the voltages stable. Figure 1 presents the shape of the instability regions. With that, the protection system will reliably detect phase-to-ground fault occurrences.

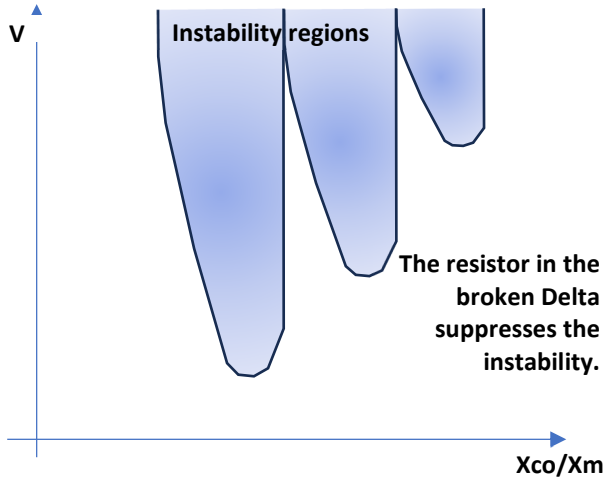

Figure 1 – Instability regions.

The first version of "Slingshot disconnection! Understanding the effect of disconnecting an un-stabilized ungrounded source" [5], made the implied assumption that the shunt capacitance to the ground would be relatively balanced. The authors concluded that if this imbalance is sufficiently large, continuous stable phase voltage imbalance would occur, quickly limiting the ability to differentiate between faulted and non-faulted conditions. As for the ferro-resonance, instabilities being mitigated by an adequately sized resistor, sizing the resistor to reduce the amount of imbalance is possible. This paper first discusses which applications could require such considerations. We then present EMT simulations and our methodology to quantify the phenomenon and the efficacy of applying specific resistor values. Next, we present the mathematical relationship that describes the simulation results. Lastly, we present the calculation steps to size the resistor to reduce the voltage imbalance reasonably.

II. APPLICATIONS

While grounded systems are more common, specific applications necessitate ungrounded configurations. As IEEE Std 142 states, [6], it has the advantage of limiting the short circuit currents for a single phase to ground fault to reduce the risk of equipment damage or for safety. Another advantage is to remove the required ground conductors. Ungrounded system conditions can also be produced unexpectedly. In both cases, carefully considering the shunt capacitance imbalance is essential for the reliable detection of phase-to-ground faults. By examining two key categories — those planned by design and those arising unexpectedly — this paper explores the implications of ungrounded bus configurations with significant shunt capacitance imbalances. Through this examination, we gain insights into the challenges and solutions associated with ungrounded power systems.

A. Application of Ungrounded Bus by Design

In power engineering, an ungrounded bus configuration is deliberately chosen for specific critical applications. One such instance is a generator bus where the generator neutrals present a large impedance to the ground. This design choice ensures the system remains operable even when one phase is grounded. An ungrounded system can tolerate a single ground fault without causing a system-wide shutdown, allowing for a controlled mitigation of the condition. In this configuration, the shunt capacitance imbalance becomes a critical consideration. The shunt capacitance imbalance naturally occurs due to manufacturing choices, where perfectly symmetrical design is impractical or cost prohibitive. For example, when building a 3-core transformer, one core is typically placed between the others. Similarly, a horizontal bus arrangement has one center phase and two sides symmetrical to each other. An overhead line built in a delta configuration has one or 2 phases closer to the ground than the other(s). This can lead to different capacitance values between phases and the ground. These differences cause an imbalance in the phase voltages with respect to the ground.

Another design-based application uses an ungrounded bus in the tertiary winding of a transformer, particularly in an autotransformer configuration. In such cases, the tertiary winding is typically delta-connected and is often used for auxiliary or instrument transformer connections. In an ungrounded system, loads must be connected phase to phase. Figure 2 depicts a plant or station auxiliary connected to an ungrounded bus. It is economical to connect a single primary winding phase-to-phase with two secondary windings phased in opposition to a grounded neutral. This configuration can create a large shunt capacitance imbalance, especially if the auxiliary transformer is connected using lengthy isolated cables.

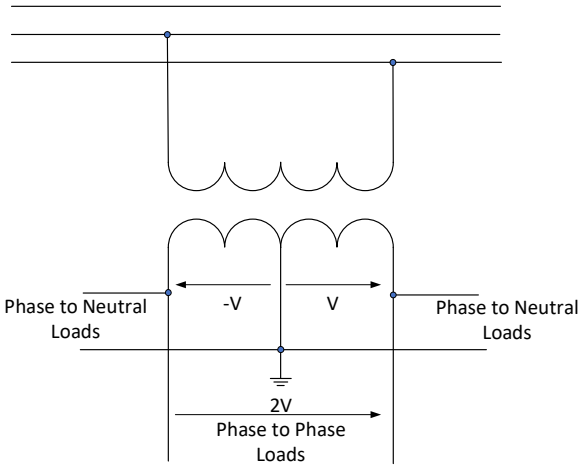

Figure 2 – Phase to Phase auxiliary transformer.

B. Unexpected Application of Ungrounded Bus

In some cases, an ungrounded bus might not be planned but may arise unexpectedly due to various factors [7], [5]. One such situation is when distributed generation, such as renewable energy sources, back-feeds into an isolated portion of a transmission system. Figure 3 presents the case when such distributed generation is connected to the system. This can create an ungrounded (and energized) condition if the substation distribution transformer is connected to the transmission system through delta winding connections. This unexpected ungrounded condition of the transmission system can be very challenging. This is why the IEEE Interconnection guide [7] invites engineers to implement first ground detection schemes. Several methods are proposed, but some use a single PT, which introduces a shunt capacitance imbalance. Also, some local loads may be single- or two-phase connected. Transmission lines feeding the station may also feed one or two phases of tap load.

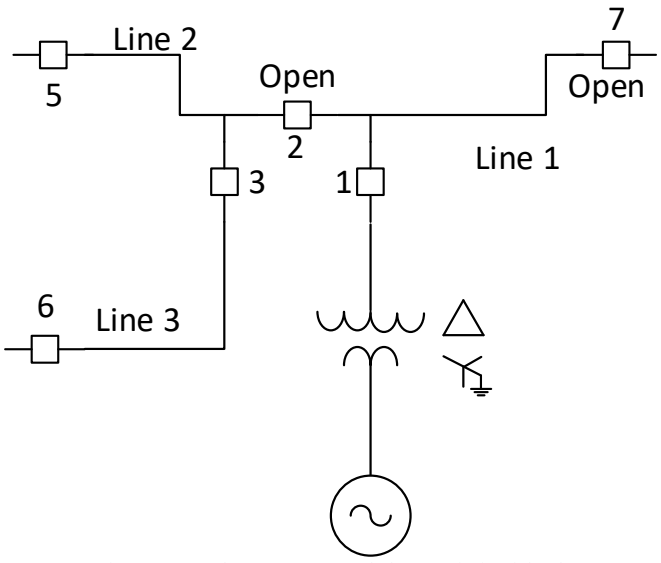

Figure 3 – Inadvertent ungrounded transmission island.

III. METHOD AND SIMULATION PLAN

In the first version of the paper [5] the authors found that two factors determine the efficiency of the resistor to reduce continuous phase imbalance. The shunt capacitance alone determines the size of the imbalance when little to no resistive power suppression is present (large resistor value on the secondary terminal of the broken delta). The average shunt capacitance alone determines the efficacy of a resistor at reducing the phase imbalance. Therefore, we sought to find the amount of continuous zero-sequence voltage with two independent functions to be multiplied by each other:

$$3V0 = f_1(C_u) \cdot f_2(C_a) \qquad \text{Equation 1}$$

Where C_a is the average shunt capacitance of the three phases in nF, and C_u in the shunt capacitance imbalance in percent:

$$C_u = 100\frac{C_h - C_l}{C_l}, \qquad \text{Equation 2}$$

$$C_a = \frac{C_{AG}+C_{BG}+C_{CG}}{3} \qquad \text{Equation 3}$$

C_h is the highest shunt capacitance to the ground of each of the three phases, and C_l is the lowest shunt capacitance to each. C_{AG}, C_{BG}, C_{CG} are the respective shunt capacitances to ground.

To estimate the function f_1, we performed an EMT sweep across an extensive range of capacitance imbalances with no resistor suppression (using a 10,000 Ohm resistor to simulate the open delta). We then found a function providing a close interpolation of recorded data. Results from earlier work [5] show that 40% shunt capacitance unbalance leads to 0.35pu of 3V0 (3 times the zero-sequence voltage). As the capacitance imbalance increases, 3V0 increases with an asymptote at 3pu. We aimed to sweep up to 90% of that value at 4000% of shunt capacitance imbalance. We then considered simple growth functions to find the best curve fit of the sampled data. The coefficients were optimized to obtain a curve fit corresponding to the minimum in the square of the differences with the sampled data. We also considered the curve produced by a 4-point polynomial (of the 3rd order) interpolation. The points were chosen based on a practical range of 100 to 1000 percent imbalance. One important practical consideration was that we do not want an estimation function that would underestimate the zero sequence voltages. The exact points chosen are such that they produce a larger estimate of the zero-sequence voltage even outside of the practical range. Some polynomial interpolation points may be slightly raised to keep the estimate above all the sampled points.

To estimate the function f_2, we performed multiple sweeps of the connected resistor impedance value for various capacitance imbalances. We then used the same curve fit methodology used for f_1 to define the function f_2. There is, however, one difference in the complexity of this task: the function has one variable shifting the curve horizontally, i.e., the average shunt capacitance to the ground C_a.

A. *Finding an interpolation estimate of the function f_1*

The EMT model used to perform the simulations is depicted in Figure 4.

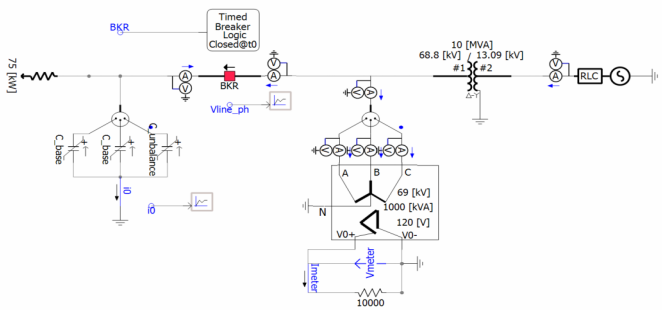

Figure 4- EMT system model - shunt capacitance sweep.

This model is simplified compared to the initial research [5] because the per-phase capacitance is a direct entry capacitor rather than a transmission line. This allows the study to control the shunt capacitance imbalance values directly. Another difference is that the source now includes a source impedance. A few trials showed that the source had a small impact on the zero-sequence content, which increased by approximately 2% when reaching a value of 75 Ohms (0.2Ω+0.2mH). Since we sought to estimate the worst-case estimation (we would rather overestimate the zero-sequence voltage content), we kept this source impedance during the entire study.

We generated 100 samples of shunt capacitance imbalance exponentially spaced between 3 and 3944% of imbalance. Phase C's first sample had 10.377nF, and the hundredth sample had 404.4nF. This was achieved by having a base capacitance of 10nF on 2 phases (A and B) and a varied capacitance of:

$$C_{unbalanced} = 0.037e^{0.01 \cdot i} \qquad \text{Equation 4}$$

Where i is the run iteration index varying from 0 to 100, increasing by one in each iteration, $C_{unbalanced}$ is assigned as the shunt capacitance for phase C. Figure 5 depicts the controls.

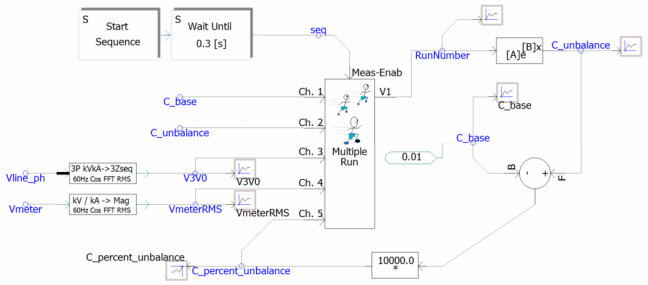

Figure 5 – Multiple-Run controls of the EMT simulation.

Recorded data include the base capacitance and the varied capacitance. The phase voltages were processed through a component that scales from kilovolt to 3 times volt and extracts the 60 Hz magnitude of the zero-sequence voltage. So, the next recorded value was 3V0 in volts. We recorded the voltage magnitude across the resistor in volts from the Vmeter. Readings were scaled from kilovolt to Volt and the 60 Hz magnitude is extracted from the FFT component. Last, we recorded the percent of shunt capacitance imbalance, as described in the model diagram.

Next, we used the data set produced using Python scripting tools to find curve fit estimations. Considering the growth

function with the shape found in our earlier work [5], we considered the following functions:

Logarithmic growth function:

$$V_{3V0pu} = a \cdot ln(b \cdot C_u + c) + d \qquad \text{Equation 5}$$

Fraction of the power function:

$$V_{3V0pu} = \frac{a \cdot C_u}{(b + {C_u}^c)^{\frac{1}{c}}} + d \qquad \text{Equation 6}$$

The polynomial interpolation:

$$V_{3V0pu} = a \cdot {C_u}^3 + a \cdot {C_u}^2 + a \cdot C_u + d \qquad \text{Equation 7}$$

The points used for this interpolation are:

C_u %	V_{3V0pu}	V_{3V0pu} adjusted
109.6	0.8046	0.8409
323	1.5661	1.5764
610	2.0295	2.0383
967	2.3137	2.3345

Table 1 – Polynomial interpolation points.

An adjustment was made visually for the purpose of avoiding the polynomial oscillations between the points that would be lower than the sampled data.

The results from the optimizations are the following:

t	a	b	c	d	Maximum error from all samples
Logarithmic	0.626073	0.244194	4.722191	-1.241454	23.58%
Fraction of the power	3.042784	304.87199	1.00000015	$-3.3605 \cdot 10^{-9}$	$2.68 \cdot 10^{-9}$%
Polynomial	$2.712278 \cdot 10^{-1}$	$5.893840 \cdot 10^{-3}$	$-6.663924 \cdot 10^{-3}$	$2.870167 \cdot 10^{-9}$	3.1%*

* Samples between 100 to 1000% capacitance unbalance.

Table 2 – Results from the estimation functions tested.

We noticed that the fraction of power function is nearly a perfect match. Also, c is nearly 1, and d is nearly 0. We can, therefore, simplify its expression through rounding. The logarithmic function is a poor match. The polynomial is a better approximation within a reduced range of applicability.

We rewrite the fraction of power to be:

$$V_{3V0pu} = \frac{3.043 \cdot C_u}{305 + C_u} \qquad \text{Equation 8}$$

The maximum error of this simplification against the recorded samples is 0.00405%, which shows that the error increased by orders of magnitude. However, it remained an accurate approximation. All the curves and the data samples are plotted in Figure 6.

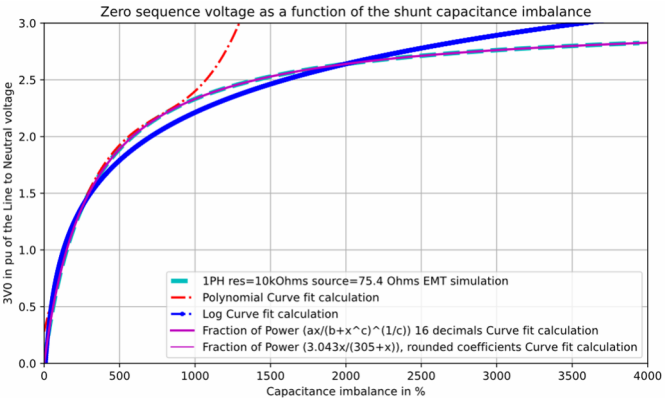

Figure 6 – Plot of recorded and interpolated zero-sequence voltage.

B. *Finding an interpolation estimate of the function f_2*

The EMT model to produce the dataset is nearly identical to the one used for the shunt capacitance imbalance sweep. It is depicted in Figure 7.

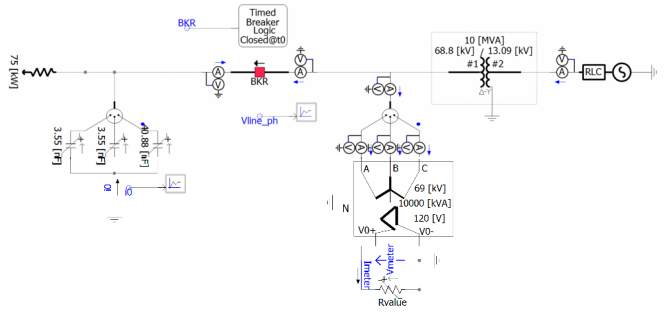

Figure 7 – EMT model used for the resistor value sweep.

In this model, the shunt capacitor values are updated manually to produce a resistor sweep at varied average capacitance and at varied shunt capacitor imbalance. We know from the previous research [5] that the average capacitance's only effect is to shift the curve inflection point horizontally. We also know that the shunt capacitance imbalance's only effect is to raise zero sequence voltages by the same factor across the range of resistor values, keeping the shunt capacitance imbalance fixed at 1050%. We performed resistance sweeps at average capacitances of 1, 2, 4, 8, and 16nF.

A resistance sweep was also performed through an exponential spacing of the sample with the following function:

$$R = 0.033e^{0.1 \cdot i} \qquad \text{Equation 9}$$

Where i is the sample index from 1 to 100. Figure 8 depicts the controls used in this model.

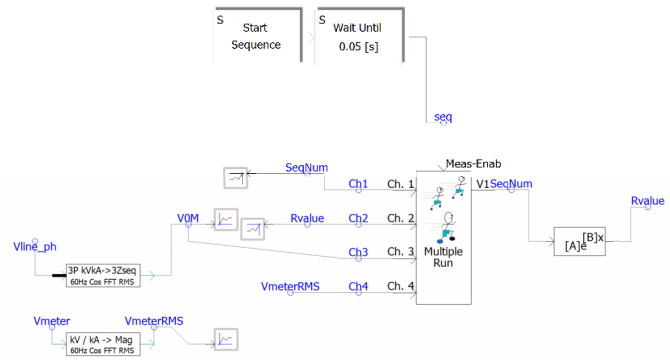

Figure 8 – Resistor sweep control of the EMT model.

As for the imbalance sweep, we recorded the iteration number, the resistor value, three times the zero-sequence voltage, and the voltage across the resistor.

We performed a curve fit at 1050% shunt capacitance imbalance and we divided the recorded data by the expected undamped maximum zero-sequence voltage given by:

$$V_{3V0pu} = \frac{3.043 \cdot C_u}{305 + C_u} \qquad \text{Equation 8}$$

We normalized the recorded samples by dividing them by the maximum content of 3V0 for an imbalance of 1050%, i.e. divided by 2.358Vpu.

Average Shunt Capacitance	Phase A and B	Phase C
1 nF	0.222 nF	2.56 nF
2 nF	0.222 nF	5.11 nF
4 nF	0.888 nF	10.22 nF
8 nF	1.777 nF	20.444 nF
16 nF	3.55 nF	40.88 nF

Table 3 – Shunt capacitance values used.

We curve fit for a fraction of the power function presented as Equation 10:

$$V_{3V0norm} = a + \frac{r}{(b^c + r^c)^{\frac{1}{c}}} \qquad \text{Equation 10}$$

We optimized the coefficients for each of the average shunt capacitance values. The results are presented in Table 4.

Average Shunt Capacitance	a	b	c	Maximum Error
1 nF	-0.00618	23.218	1.8299	1.41%
2 nF	-0.0084	11.526	1.834	1.38%
4 nF	-0.0101	5.7233	1.847	1.33%
8 nF	-0.0104	2.8558	1.8741	1.14%
16 nF	-0.00994	1.4230	1.9021	0.92%

Table 4 – Optimization of coefficients R sweep.

Table 4 shows that the function type is a good match for the sampled data with an error maximum of around 1%. We also see that the coefficient can be forced to be 0 and that the c coefficient is trending towards 2. So, we re-optimized based on b with a=0 and c=2.

Average Shunt Capacitance	a	b	c	Maximum Error
1 nF	0	24.968	2	1.93%
2 nF	0	12.4937	2	1.94%
4 nF	0	6.2229	2	1.86%
8 nF	0	3.0832	2	1.59%
16 nF	0	1.5197	2	1.29%

Table 5 – Simplified optimization parameters.

Table 5 shows that forcing a=0 and c=2 did not significantly increase the maximum error, which stays below 2% for 1nF and greater.

Next, we found a function that fits five values of b for each average capacitance value. A possible good match for these points is the function presented in Equation 11.

$$b = \frac{a}{{C_a}^b} \qquad \text{Equation 11}$$

The optimization produced the following results, a= 24.978 and b=1.002755, with a maximum error of 1.944%. We re-ran the error calculation with a=$\sqrt{600}$=24.49 and b=1, and the error was marginal at 0.31%.

Using Equation 8 and Equation 10, we found that the 3V0 can be calculated with this function presented in Equation 12.

$$V_{3V0pu} = \frac{3 \cdot C_u}{305 + C_u} \cdot \frac{r}{\sqrt{\frac{600}{{C_a}^2} + r^2}} \qquad \text{Equation 12}$$

We graphed the performance of Equation 1, as a resistor sweep against the corresponding data for a few values of average capacitance as well as percent imbalance.

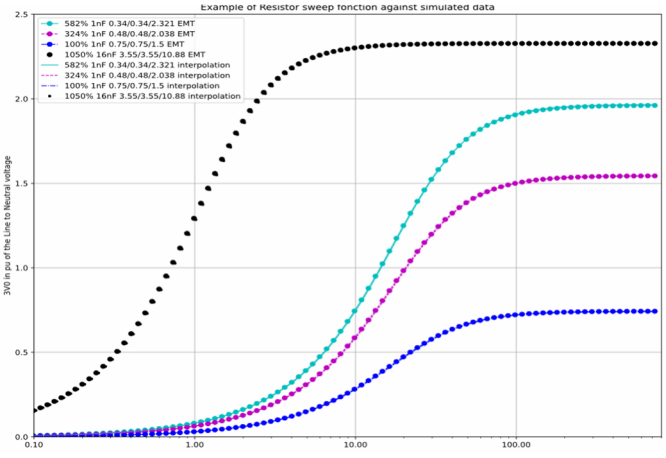

Figure 9 – 4 examples of the curve fit performance.

Figure 9 Shows the performance of the curve fit equations we created. The maximum error on the 400 points represented on these four estimation curves is 0.347%.

IV. The Mathematical relationship To estimate the resistor value.

We can find the expression of R based on a desired maximum zero-sequence content on the phase by solving for r in Equation 12.

$$r = \frac{\sqrt{600}\cdot V_{3V0m}}{C_a\cdot\sqrt{1-{V_{3V0m}}^2}} \qquad \text{Equation 13}$$

$$\textit{Where}\quad V_{3V0m} = \frac{V_{3V0pu}\cdot(305+C_u)}{3\cdot C_u} \qquad \text{Equation 14}$$

V_{3V0pu} is the desired amount of 3VO in per unit of the line-to-line voltage.

V. Conclusion

We have defined a mathematical relationship allowing engineers to estimate the expected continuous content of zero-sequence voltage in the phase voltage in reference to ground. One important component is still missing to help the engineer size the resistor. The engineer also needs knowledge of how much zero-sequence voltage is allowed in the phase voltages. Typically, this application is designed with a potential transformer rated primary equal to the line-to-line voltage, so in theory, there is no insulation requirement to limit the zero-sequence content. The scheme is, however, installed for ground fault detection, making it important to keep the zero-sequence voltage content low enough to allow for a clear distinction between faulted and non-faulted conditions. For this purpose, limiting the unfaulted zero-sequence voltage to 30% seems like a decent choice. But we must also remember that the value chosen should avoid unstable regions described in [8].

VI. Bibliography

[1] IEEE Guide for Protective Relay Applications to Power System Buses, IEEE C37.234, 2021.

[2] R. Karlicek and E. R. J. Taylor, "Ferroresonance of Grounded Potential Transformers on Ungrounded Power Systems," *IEEE Trans Part III Power Apparatus and Systems,* vol. 78, no. August, pp. 607-614, 1959.

[3] H. S. Scott and P. H. A., "Criteria for Stability of Wye-Grounded-Primary Broken Delta Secondary Transformer circuits," *Ibid,* vol. 60, no. Nov 1941, pp. 997-1002, 1941.

[4] C. T. Weller, "Experiences with Grounded-Neutral, Y-Connected Potential Transformers on Ungrounded Systems," *Transactions of the American Institute of Electrical Engineers,* vol. 50, no. March 1931, pp. 299-316, 1931.

[5] S. Billaut, J. Johnson, A. Miles, James Steele, K. Banerjee and S. Miller, "Slingshot Disconnection! Understanding the effect of disconnecting an un-stabilized, ungrounded source," in *PACworld Americas 2023*, Raleigh, 2023.

[6] IEEE, Green Book IEEE Std 142, IEEE, 1991.

[7] K. Behrendt, "Protection for unexpected Delta Source," SEL, Spokane, 2002.

[8] H. S. Shott and H. Peterson, "Criteria For Neutral Stability of Wye-grounded-Primary Broken-Delta Secondary Transformer circuits," *AIEE (IEEE) Transactions,* vol. 60, no. November, pp. 997-1002, 1941.

[9] *The 59N and Broken Delta Applications,* Highland, IL: Basler Electric,.

[10] G. Johnson, M. Schroeder and G. Dalke, A Review of System Grounding Methods and Zero Sequence Current Sources, Highland, IL.: Basler Electric Company.

[11] "https://voltage-disturbance.com/power-engineering/neutral-inversion-and-neutral-displacement/," Voltage Disturbance Power Engineering Expert. [Online].

[12] IEEE Standard for Interconnecting Distributed Resources with Electric Power Systems, IEEE1547, 2018.

[13] *Neutral Grounding Resistors Technical Information,* Erlanger, KY: Post Glover.

[14] J. L. Blackburn, Protective Relaying, Fourth Edition., CRC Press, 2014.

[15] IEEE Guide for Protective Relaying of Utility-Consumer Interconnections, IEEE C37.95, 2014.

Sebastien Billaut, PE is a consulting engineer at Commonwealth Associates. Mr. Billaut holds an MS in Mechanical and Electrical Engineering from ESTP in France. He has 31 years of utility-related engineering experience, setting protection relays and power system modeling. He is the patent author of microgrid fault management technology. He also co-authored a patent on substation battery life extension during station outages.

He participates in industry-wide microgrid, distribution, and transmission protection systems standards. He serves as Chair of the IEEE PSRC Working Group K29, D44, KTF33, and K52 and is a member of IEEE PSRC Main and Subcommittees D and K. He is currently contributing to IEEE 1547.x and IEEE 2800.x

James Steele, E.I.T., is a substation engineer at Commonwealth Associates. He has two years of utility experience. He graduated from Michigan Tech with a Bachelor's in Mechanical Engineering and a Master's in Electrical Engineering. James' experience is in protection and control, with an emphasis on relay settings. He has completed many substation projects, including those for data centers and solar farms. In addition to his design experience, he has ten years of experience as a submarine electrician.

Koustubh Banerjee, PE is an Electrical Engineer in the Electrical Systems Studies department at Commonwealth Associates, Inc., in Jackson, Michigan. He received his bachelor's degree in electrical engineering from NIT Kurukshetra, India, in 2011, and his master's degree, also in electrical engineering, from Arizona State University in 2014. He has been in the power industry for more than 5 years. At Commonwealth, he has worked on various relay settings and protection coordination projects for utilities. He is also experienced in transmission planning and NERC MOD and PRC compliance studies. Koustubh is registered as a Professional Engineer (PE) in the State of Michigan.

Joseph Johnson, P.E., is a seasoned electrical engineer who graduated from Michigan Technological University in 2015 with a Bachelor's degree in Electrical Engineering. Specializing in relay protection settings and system studies, Joseph's expertise spans voltages of up to 500kV, where he has devised intricate protection schemes for critical components, including transmission lines, buses, transformers, feeders, and capacitors.

Since delving into inverter-based resources in 2020, Joseph has actively contributed to developing and optimizing five battery energy storage systems and four inverter-based collection systems, ranging from 150 to 500 MVA. With a passion for engineering and a knack for innovation, Joseph is dedicated to advancing renewable energy technologies and tackling complex challenges in the field.

Mr. Miller has over 40 years of experience in the analysis and planning of electric utility transmission systems and the design and development of associated software programs. As a consultant, Mr. Miller has been responsible for assisting generators with the interconnection process. These include dozens of proposed renewable projects all across the U.S. Occasionally, these projects materialize and, when they do, the interconnection concepts developed by Mr. Miller and his colleagues have been implemented. Outside of his interconnection expertise, Mr. Miller has three engineering degrees from the University of Michigan. He has performed all manner of study projects involving the grid, ranging from cascade failure analysis, generation adequacy, and protection studies, to economics studies and special studies. Mr. Miller works successfully at the boundary of engineering and legal, regulatory, and business issues, successfully developing and presenting testimony and positions.